From www.bloodjournal.org by guest on January 12, 2018. For personal use only.
Blood First Edition Paper, prepublished online November 29, 2017; DOI 10.1182/blood-2017-08-800359

The BEACH-domain containing protein, Nbeal2, interacts with Dock7, Sec16a and Vac14

Running head: Biochemical interactions of Nbeal2

Louisa Mayer[1,2], Maria Jasztal[1,2], Mercedes Pardo[3*], Salvadora Aguera de Haro[1,2], Janine Collins[1,2,4], Tadbir K Bariana[1,5,6], Peter A Smethurst[1,2], Luigi Grassi[1,2], Romina Petersen[1,2], Paquita Nurden[7], Rémi Favier[8,9], Lu Yu[3*], Stuart Meacham[1,2], William J Astle[10], Jyoti Choudhary[3*], Wyatt W Yue[11], Willem H Ouwehand[1,2,3], Jose A Guerrero[1,2]**

[1]Department of Haematology, University of Cambridge, Cambridge Biomedical Campus, Cambridge, UK.
[2]National Health Service Blood and Transplant, Cambridge Biomedical Campus, Cambridge, UK.
[3]Wellcome Trust Sanger Institute, Wellcome Trust Genome Campus, Hinxton, Cambridge, UK.
[4]Department of Haematology, Barts Health National Health Service Trust, London, UK.
[5]Katharine Dormandy Haemophilia Centre and Thrombosis Unit, Royal Free London NHS Foundation Trust, London, UK.
[6]Department of Haematology, University College London Cancer Institute, London, UK.
[7]Institut Hospitalo-Universitaire L'Institut de Rythmologie et Modelisation Cardiaque, Hopital Xavier Arnozan, Pessac, France.
[8]Département d'Hématologie, Assistance-Publique Hôpitaux de Paris, Centre de Référence des Pathologies Plaquettaires, Hôpital Armand Trousseau, Paris, France.
[9]Institut National de la Santé et de la Recherche Médicale U1170, Villejuif, France.
[10]MRC/BHF Cardiovascular Epidemiology Unit, Department of Public Health and Primary Care, University of Cambridge, Strangeways Research Laboratory, Wort's Causeway, Cambridge, UK.
[11]Structural Genomics Consortium, Nuffield Department of Clinical Medicine, University of Oxford, Oxford, UK.

Copyright © 2017 American Society of Hematology

From www.bloodjournal.org by guest on January 12, 2018. For personal use only.

*Current address: The Institute of Cancer Research, Cancer Biology Division, Chester Beatty Laboratories, London, UK.

**Current address: EMBL European Bioinformatics Institute, Wellcome Trust Genome Campus, Hinxton, Cambridge, UK.

Correspondence to:

Jose A Guerrero (jg652@medschl.cam.ac.uk)

Department of Haematology, University of Cambridge

Long Road, CB2 0PT, Cambridge, UK.

Tel: +44 1223 588095 // Fax: +44 1223 588155

Text Word Count: 3,913 // Abstract Word Count: 184 // Number of Figures: 6 //

Number of References: 56

Scientific category: Platelets and Thrombopoiesis

Key Points:

- Nbeal2 interacts with Dock7, Sec16a and Vac14 and missense variants causing Gray Platelet Syndrome disrupt the binding of Dock7 and Vac14.
- The level of the α-granule protein Dock7 in platelets from *Nbeal2*$^{-/-}$ mice and GPS cases is reduced and its signaling pathway is dysregulated.

From www.bloodjournal.org by guest on January 12, 2018. For personal use only.

Abstract

Mutations in *NBEAL2*, the gene encoding the scaffolding protein Nbeal2 are causal of Gray Platelet Syndrome (GPS), a rare recessive bleeding disorder characterized by platelets lacking α-granules and progressive marrow fibrosis. We present here the interactome of Nbeal2 with additional validation by reverse immunoprecipitation of Dock7, Sec16a and Vac14 as interactors of Nbeal2. We show that GPS-causing mutations in its BEACH domain have profound and possible effects on the interaction with Dock7 and Vac14, respectively. Proximity ligation assays show that these two proteins are physically proximal to Nbeal2 in human megakaryocytes. In addition, we demonstrate that Nbeal2 is primarily localized in the cytoplasm and Dock7 on the membrane of or in α-granules. Interestingly, platelets from GPS cases and *Nbeal2*$^{-/-}$ mice are almost devoid of Dock7 resulting in a profound dysregulation of its signaling pathway, leading to defective actin polymerization, platelet activation and shape change. This study shows for the first time proteins interacting with Nbeal2 and points to the dysregulation of the canonical signaling pathway of Dock7 as a possible cause of the aberrant formation of platelets in GPS cases and *Nbeal2* deficient mice.

From www.bloodjournal.org by guest on January 12, 2018. For personal use only.

Introduction

Cellular secretion is a key biological event involved in many physiological processes including hemostasis [1,2]. Secretory cells store granules, which are released according to predetermined temporal and spatial programs [3]. The function of secretory cells is to a large extent linked to their types of granules, their content and the signaling events leading to secretion. Therefore the ontology and homeostasis of granules must be highly regulated, i.e. from the formation of the vesicles themselves and cargo sorting through cytoplasmic maintenance of formed vesicles and eventual exocytosis [4,5]. Blood platelets are anucleated secretory cells originating from megakaryocytes (MKs) [6]. Their primary role is in hemostasis [7], but they are also relevant in other patho-physiological pathways [8-12]. Platelet function is mediated by the release of their three types of granules upon vascular injury [13]. Aberrations in any of these three granule types lead to inability of platelets to sustain hemostasis, resulting in bleeding [14]. Defects in lysosomes are observed in Chediak-Higashi Syndrome and caused by mutations in *LYST* encoding a member of the family of Beige and Chediak-Higashi (BEACH)-domain (BEACH hereafter) containing proteins [15]. Aberrations of platelet δ-granules are observed in Hermansky-Pudlak syndrome caused by mutations in 11 genes encoding proteins with roles in the formation and trafficking of granules [16]. Haploinsufficiency of another BEACH family member, *Neurobeachin* (*NBEA*), is associated with severe autism and atypical δ-granules in humans [17] and *Nbea* heterozygous mice [18].

The α-granules are the most abundant organelles and granules in platelets. They contain hundreds of proteins with important functions in hemostasis and wound healing [8-12,19]. Loss of function variants of the BEACH-domain gene *NBEAL2* in Gray Platelet Syndrome (GPS) cases leads to absence of platelet α-granules [20-23]. *Nbeal2*$^{-/-}$

From www.bloodjournal.org by guest on January 12, 2018. For personal use only.

mice present with a faithful copy of human GPS with the typical large platelets of grayish appearance and interestingly neutrophils and mast cells are also dysfunctional [24,25]. *In vivo* studies highlight the role of *Nbeal2* beyond hemostasis, particularly in inflammation, innate immunity and cancer [24,26-28]. However, the molecular function of Nbeal2 protein has not been explored.

The BEACH proteins Lyst, Nbea and Nbeal2 are deemed essential for molecular processes underlying the formation, retention and secretion of the three types of granules in platelets [29]. All nine BEACH genes encode large proteins between 2,000 – 4,500 residues containing the Armadillo-type, Concanavalin-A lectin, Pleckstrin Homology (PH) and WD40 repeat domains in addition to the typical BEACH domain [29]. This domain of approximately 35 kDa is unique to the BEACH family, highly conserved in eukaryotes and does not share sequence homology with other proteins [15]. It is characterized by a unique hydrophobic secondary structure that cannot be classified as either β-strands or random coils [30] and strongly interacts with its neighboring PH domain but the significance of this interaction remains elusive [31]. Here we use expression of Nbeal2 domains in human cells to define its proximal interactome with confirmation of Dock7, Sec16a and Vac14 as Nbeal2 binding partners by different biochemical and cellular approaches. We show that GPS-causing mutations strongly reduce the interaction of Dock7 with the BEACH domain and platelets from *Nbeal2*$^{-/-}$ mice and GPS patients are nearly devoid of Dock7 with a direct impact on platelet function.

Material and Methods

Short descriptions of the methods used are provided in this section and complete details are given in supplemental methods.

From www.bloodjournal.org by guest on January 12, 2018. For personal use only.

Cell culture and stable clones

Human Embryonic Kidney 293T cells (HEK) and CHRF-288 cells (CHRF) were cultured following AATC procedures. Stable transfectants ectopically expressing the protein domains under study were generated by infection with lentiviral particles. HEK were transduced at a Multiplicity Of Infection (MOI) of 10 Transducing Units (TU) per cell in the presence of 1 µg/mL polybrene. CHRF were transduced at an MOI of 50 TU/cell in the presence of 1 µg/mL protamine sulfate.

Tandem affinity purification

Cells were collected, washed twice with cold PBS and pellets were snap-frozen on dry-ice and kept at -80ºC until immunoprecipitation. Pellets were resuspended with lysis buffer containing 0.1% NP-40 and protease inhibitor cocktail. Tandem affinity purification and sample preparation for mass spectrometry analysis were performed as previously described [32].

Mass spectrometry and data analysis

Peptides were re-dissolved in 0.5% formic acid and analysed with on-line nano liquid chromatography tandem mass spectrometry on an LTQ FT mass spectrometer (Thermo-Fisher Scientific) coupled with an Ultimate 3000 Nano/Capillary LC System (Dionex). Proteins frequently identified from tandem affinity purifications of unrelated targets in embryonic stem cells were discarded.

The mass spectrometry proteomics data can be retrieved from the ProteomeXchange Consortium via the PRIDE [33] partner repository with the dataset identifier PXD006091.

From www.bloodjournal.org by guest on January 12, 2018. For personal use only.

Immunoprecipitation of endogenous proteins

Total cell lysates were generated as above and proteins of interest were immunoprecipitated using Protein G Dynabeads (Invitrogen) and selected antibodies.

Proximity Ligation Assays

Human MKs were generated from $CD34^+$ hematopoietic stem cells as stated in supplemental methods. Proximity ligation assays (PLAs) were performed following the manufacturer's protocol.

Mice

Adult animals were used including age-matched controls of the same genetic background. This study has been regulated under the Animals (Scientific Procedures) Act 1986 Amendment Regulations 2012 following ethical review by the University of Cambridge Animal Welfare and Ethical Review Body (AWERB) (Home Office PPL70/8406). A minimum of 5 different mice per experiment was used unless otherwise stated.

Isolation of platelets

Mouse blood was withdrawn from the inferior vena cava in either EDTA (5mM final) or ACD (111 mM glucose, 71 mM citric acid, 116 mM sodium citrate) while blood from GPS patients and controls was taken as previously reported [21]. In both cases, platelets were washed using Tyrode's buffer pH 6.5.

Immunoblots

From www.bloodjournal.org by guest on January 12, 2018. For personal use only.

HEK, CHRF and platelets were lysed by addition of FTAP-lysis buffer (0.1% NP-40, 150 mM NaCl, 10 mM Tris, pH 8) containing protease inhibitor cocktail and incubated on ice for 10 min before centrifugation at 13000 rpm for 15 min at 4ºC.

Analysis of active Cdc42 and Rac1

Platelets were washed as above and adjusted to $3x10^5$ platelets/µL in Tyrode's buffer pH 7.35. Stimulations with vehicle (PBS) and thrombin (T4648, Sigma, UK) were done at RT for different time points and lysis buffer provided by assay kit (BK127 and BK128, Cytoskeleton, US) was added. Subsequent steps were carried out following the manufacturer's protocol. Absorbance at 490 nm was read using an MP5 plate reader (Molecular Devices, UK).

F-actin formation in platelets

Washed platelets were activated for 10 min and then fixed, permeabilized, incubated with 488-Phalloidin for 20 min and read in a Gallios flow cytometer (Beckman Coulter, UK).

Platelet spreading on fibrinogen

A solution of 100 µg/mL of fibrinogen (FIB3, Enzyme Research, UK) in PBS was used to coat coverslips (12392128, Thermo-Fisher Scientific) overnight at 4ºC. Platelets at $5x10^3$/µL in Tyrode's buffer pH 7.35 were seeded onto the coverslips and platelet agonists or vehicle were added.

Transmission electron microscopy and gold-labeling

From www.bloodjournal.org by guest on January 12, 2018. For personal use only.

Cells were harvested, washed in physiological saline solution and fixed in 2% glutaraldehyde and 2% formaldehyde in 0.05M cacodylate solution, pH 7.4 for 4-6 hours at 4ºC [27]. Platelets were labelled as previously reported [34].

Confocal microscopy

Cells grown on coverslips were fixed with 2% paraformaldehyde-PBS for 30 min at RT and washed twice with PBS.

Statistics

Results are shown as mean ± SEM. Statistical analysis was performed using the unpaired Student's t test. p-values<0.05 were considered statistically significant.

A complete list of primary antibodies used in this study is provided in Table S1.

RESULTS

The Nbeal2 interactome

To identify the putative interacting proteins of Nbeal2 (the interactome hereafter) a construct encompassing the PH, BEACH and WD40 (PBW) domains and a FLAG Tandem Affinity Purification (FTAP) tag [32] (Figure 1A) was used to transform HEK (Figure 1B), which endogenously express Nbeal2 (Figure S1A). An FTAP-tagged green fluorescent protein (GFP) construct was used as a control (Figure 1A and 1B). Cells were then used in a two-step (FLAG and calmodulin binding peptide) sequential affinity purification and the resulting eluate was separated by SDS-PAGE followed by mass spectrometry analysis (Figure 1C). Proteins identified in GFP samples and from

From www.bloodjournal.org by guest on January 12, 2018. For personal use only.

an “in-house contaminant” database as stated in Methods were removed from further analysis. The classification of the remaining 132 proteins (129 entries by gene name excluding *NBEAL2*; Table S2) according to the most frequent gene ontology terms shows an array of biological functions (Figure 1D).

To better comprehend its functional role, we used the interaction data to embed Nbeal2 in a protein-protein interaction network (PPIN) representing the processes of hemostasis, megakaryopoiesis and platelet formation [35]. The PPIN of 5,112 nodes (proteins) and 27,441 edges (biochemical interactions) was obtained by retrieving first order interactions from Reactome [36] and IntAct [37] using a set of 637 bait proteins (baits hereafter). The set of genes encoding the baits resulted from an integrative analysis of a genome wide association study (GWAS) for platelet traits in 173,480 individuals [38,39] and a promoter capture Hi-C assay in human MKs [40]; the 79 genes implicated in Mendelian disorders of hemostasis were also included [14,41]. Of the 129 nodes in the Nbeal2 interactome, 91 are present in the PPIN (orange nodes in Figure 1E) and the remaining 38 are first order interactors with one or several proteins of the PPIN (purple nodes in Figure 1E).

Previous studies on proteins from the BEACH family suggest that they may function as scaffolds with a critical role of Nbeal2 in homeostasis of α-granules [26,27,29]. Based on this and on a detailed inspection of the PPIN, 10 candidate proteins were selected for validation studies by reverse immunoprecipitation (Table S2) and the interactions of three proteins were confirmed, namely Dock7 (a guanidine exchange factor [GEF]); Sec16a (an endoplasmic reticulum [ER] membrane protein); and Vac14 (a regulator of phosphatidyl inositol 3,5- bisphosphate [PtdIns[3,5]P2]) (triangular

From www.bloodjournal.org by guest on January 12, 2018. For personal use only.

orange nodes in Figure 1E). Their first order interactors are illustrated in the subnetworks in Figure 1F-1H (Figure S2-S4 for fully-labeled versions).

Dock7, Sec16a and Vac14 interact with Nbeal2

To confirm the interactions with Nbeal2, we firstly performed immunoprecipitation of the selected candidates in PBW-FTAP HEK and positive results for Dock7, Sec16a and Vac14 were obtained (Figure 2A and 2B). These experiments showed that endogenous Sec16a and Vac14 pulled-down PBW-FTAP and Dock7, and endogenous Dock7 pulled-down PBW-FTAP and Vac14 (Figure 2B, Figure S5). Assays in GFP-FTAP HEK, as expected, showed no interactions with any of the three proteins (Figure 2C). Secondly, we used CHRF, which have a transcriptome reminiscent of MKs [42] and a robust Nbeal2 protein expression (Figure S1B). Lentiviral transduction with PBW-FTAP followed by the same experimental approach as used for HEK confirmed the interaction with Dock7, Sec16a and Vac14 in PBW-FTAP CHRF (Figure 2D). Furthermore, endogenous Nbeal2 was also detected when the three interactors were pulled-down in non-transduced CHRF, although the recovery levels for Dock7 and Sec16a were low (Fig 2E). Finally, after the initial successful validation experiments with cell lines, we used PLA in MKs derived from human hematopoietic stem cells [43]. The two most abundant platelet membrane receptor complexes for fibrinogen (αIIbβ3 integrin) and Von Willebrand Factor (GPIbα, GPIbβ, GPV, GPIX) respectively were used to validate the assay. As expected, targeting αIIb and GPIX simultaneously produced a weak PLA signal similar to that using isotype controls, while targeting GPIbα and GPIX generated a strong signal (Figure 2F). When compared to the negative control, we observed a significant

From www.bloodjournal.org by guest on January 12, 2018. For personal use only.

increase in PLA signals in Dock7-Nbeal2 and Vac14-Nbeal2 labelled-MKs further supporting the interactions between these proteins (Figure 2F).

Dock7 and Vac14, but not Sec16a bind the BEACH domain

The BEACH domain intimately interacts with its adjacent amino-terminal PH domain over an interface of 1,300 $Å^2$, suggesting they may fold as a single functional unit [30,31]. We therefore overexpressed a construct comprising both the PH and BEACH domains (PB) in HEK (Figure 3A). Dock7 and Vac14 were present in PB-FTAP and PBW-FTAP pulldowns while Sec16a was recovered only with PBW-FTAP (Figure 3B). Hence, the binding of Sec16a to Nbeal2 may be mediated through the WD40 domain, whilst the other two proteins bind to either the PH and/or BEACH domain.

Impact of GPS-causing variants on the interaction of Dock7 and Vac14

To determine the possible effects of GPS-causing mutations we catalogued all reported missense variants (n=22) [21,23,44,45] and those identified "in-house" by the ThromboGenomics [41] and NIHR BioResource sequencing projects (n=14; unpublished). This showed a significant 5-fold enrichment (Fisher-test, p-value=$3.64x10^{-5}$) of variants in the BEACH domain, which harbored 13 of 36 of the observed variants (36%), whilst the domain only accounts for 292 of the 2,754 (11%) amino acids of Nbeal2. We used the coordinates of the crystal structure of the BEACH domain of Lrba (pdb 1T77) to estimate the functional consequences of the 13 mutations and selected 6 with different types of structural changes to determine their effects on the binding of Dock7 and Vac14 (Figure 3C and 3D). HEK were stably transfected with PBW-FTAP constructs and the reference and five variant-carrying baits were expressed at similar levels, indicating a minimal, if any, detrimental effect

From www.bloodjournal.org by guest on January 12, 2018. For personal use only.

of each variant on the folding of the domains (Figure 3E). Our results showed that M2080K, P2100L and G2290W/E2294G (both on the same haplotype) seemed to diminish the binding of Vac14 (Figure 3E), P2100L and R2172H significantly reduced Dock7 binding and its binding to the G2290W/E2294G bait seemed to be at a reduced level, although the difference with the reference bait was not significant (Figure 3F).

Localization of PBW-FTAP and Nbeal2 by electron and confocal microscopy

Currently, the subcellular localization of Nbeal2 remains unknown. We investigated this using PBW-FTAP CHRF by labeling its FLAG epitope. Transmission electron microscopy revealed the presence of intracellular vesicles, mitochondria and Golgi in CHRF (Figure 4A and 4B). Labeling of FLAG by gold-adsorbed immunoglobulins did not show any staining in CHRF (not shown). However, clusters of gold were observed across the cytoplasm of PBW-FTAP CHRF suggesting a cytosolic localization of PBW (Figure 4C-4F). This pattern was also confirmed by confocal microscopy by labeling PBW and F-actin with anti-FLAG and Phalloidin, respectively (Figure 4G and Figure S6). The use of a rabbit antiserum revealed the presence of Nbeal2 in the cytoplasm (arrowheads), in close proximity to enclosing membranes of the α-granules (arrows), the open canalicular system (OCS) (circles) and the cell surface (flat ellipses) of human platelets (Figure 4H).

Subcellular localization of Nbeal2, Dock7, Sec16a and Vac14 in platelets

We further investigated the localization of Nbeal2 and its interactors Dock7, Sec16a and Vac14 by subcellular fractionation of platelets. We firstly fractionated human platelets and identified cytoskeleton and dense tubular system (DTS) in fractions 1 to

From www.bloodjournal.org by guest on January 12, 2018. For personal use only.

4 (enriched for tubulin, actin and calreticulin) and α-granules in fraction 7 and 8 (enriched for the α-granule protein Thrombospondin-1 [Thbs1]) (Figure 5A). Nbeal2 was mostly found in fractions 2-4 containing cytoskeletal and DTS proteins (Figure 5A). Fractionation of murine platelets showed a similar pattern, i.e. Nbeal2 was primarily found in fractions 3-4 (Figure 5B). As expected, proteins typically stored in α-granules, Thbs1 and vascular endothelial growth factor (Vegf), are significantly reduced in GPS platelets (Figure 5B). Dock7 was present in the α-granule-containing fraction (7-8) of control platelets but was mislocalized in fraction 4 in *Nbeal2*$^{-/-}$ platelets (Figure 5C). Although at lower levels, Dock7 and Nbeal2 colocalize in fractions 3-4 and 7-8, respectively, providing further evidence of their interaction (Figure S7). The localization of Sec16a and Vac14 did not differ significantly between platelets from both groups (Figure 5D and 5E), despite potential apparent increased levels of Sec16a in *Nbeal2*$^{-/-}$ platelets (Figure 5D), an observation which was not replicated in whole platelet lysates (Figure 5F and 5G).

Having identified the impact of the absence of Nbeal2 on the subcellular localization of Dock7, we then asked whether it had an effect on the overall cellular abundance of the three interactors. Similar levels of Sec16a and Vac14 were confirmed in platelets from both groups, but the Dock7 protein level was significantly reduced in *Nbeal2*$^{-/-}$ platelets (Figure 5F, 5G and Figure S8), and importantly, also in the platelets of two GPS cases (Pedigree C of previous report [21]) (Figure 5H). Transcript levels of *Dock7* in mouse MKs did not differ significantly between control and *Nbeal2*$^{-/-}$ mice ([27] and Table S3) and immunoblots with anti-Dock7 did not reveal signs of proteolysis or higher Dock7 levels in plasma (not shown), suggesting that the Nbeal2 protein is likely involved in its post-translational modification and/or stability.

From www.bloodjournal.org by guest on January 12, 2018. For personal use only.

The Dock7 signaling pathway is altered in *Nbeal2*$^{-/-}$ platelets

As a GEF, Dock7 exchanges GDP for GTP on Cdc42 and Rac1 causing their activation, followed by activation of downstream effectors including the dephosphorylation (activation) of cofilin, a key regulator of actin turnover [46,47]. Actin reorganization then leads to extension of filopodia and generation of lamellipodia [46], ultimately resulting in platelet shape change. Given the significant reduction of Dock7 levels and its altered localization in *Nbeal2*$^{-/-}$ platelets, we postulated that this canonical signaling pathway may be disrupted and set out to test this using control and *Nbeal2*$^{-/-}$ platelets.

Firstly, the phosphorylated (inactive) form of cofilin, P-cofilin, was significantly increased in murine *Nbeal2*$^{-/-}$ platelets (Figure 6A and 6B). Other regulators of this signaling pathway such as Cdc42, Rac1, Iqgap1 and chronophin [46,48] were also measured and we found that the level of Iqgap1, a protein that stabilizes the active forms of Cdc42 and Rac1, was also significantly higher in *Nbeal2*$^{-/-}$ platelets (Figure 6A and 6B) suggesting that the increase in P-cofilin was likely due to an imbalance not only of Dock7 but also of Iqgap1. In fact, our previous gene expression array of control and *Nbeal2*$^{-/-}$ MKs revealed a significantly increased *Iqgap1* transcript level in the latter ([27] and Table S4), which is validated at the protein level in platelets in this study.

We then asked if the disequilibrium in the Dock7/Iqgap1/P-cofilin pathway had an effect on the function of platelets. Firstly, levels of active Rac1 at 2 min after activation by thrombin were significantly higher (p-value=0.026) in platelets from control versus *Nbeal2*$^{-/-}$ mice and a similar trend was observed for Cdc42, but this did not reach significance (Figure 6C and 6D). Secondly, we measured F-actin formation in platelets. Despite higher levels of F-actin in basal *Nbeal2*$^{-/-}$ platelets due to their

From www.bloodjournal.org by guest on January 12, 2018. For personal use only.

larger size (Figure 6E, p-value=0.048), induction of actin polymerization by thrombin revealed a lower increase in *Nbeal2*$^{-/-}$ platelets (Figure 6E and 6F, p-value=0.0005). At last, we checked the endpoint of this pathway i.e. platelet shape change by measuring the ability of platelets to spread onto fibrinogen after activation with both ADP and thrombin. Enumeration of activated versus non-activated platelets assessed by shape-change and spreading revealed that nearly all control platelets became activated while the *Nbeal2*$^{-/-}$ platelets showed significantly reduced spreading (Figure 6G and 6H, p-value=<0.0005). Altogether, these results are compatible with the notion that Nbeal2 plays an important role in the regulation of cytoskeletal rearrangements in platelets, most likely through its interaction with Dock7.

Discussion

Despite the severity of inherited granule pathologies caused by mutations in *NBEAL2*, *NBEA* and *LYST*, the key roles of the encoded BEACH proteins in the ontogeny of α-, δ- and lysosomal granules remain poorly defined. Here we report the results of studies aiming at defining the role of Nbeal2 at the biochemical and cellular level.

We identified the putative interactors of Nbeal2 in human cells and selected 10 candidate interactors for validation. The interactions of Dock7, Sec16a, and Vac14 with Nbeal2 were confirmed and the physical proximity of the former two to Nbeal2 in human MKs was corroborated by PLA. Furthermore, the introduction of GPS-causing mutations in the BEACH domain showed profound effects on the interactions with Dock7. While Nbeal2 is mostly present in the platelet cytoplasm, Dock7 localizes to the α-granules and, interestingly, murine and human platelets devoid of

From www.bloodjournal.org by guest on January 12, 2018. For personal use only.

functional Nbeal2 showed strongly reduced Dock7 levels resulting in changes in its canonical signaling pathway.

The 5-fold enrichment of GPS-causing variants in the BEACH domain prompted us to perform the pull-downs with a construct containing the BEACH and its PH and WD40 flanking domains. Despite the potential presence of false-positive interactors, frequently seen in proteomics assays, 70% of the 129 proteins in Nbeal2's interactome are present as primary nodes in the PPIN, which represents a lion's share of the proteome of human MKs. So far no similar interaction data are available for any of the BEACH proteins, except for the 21 proteins possibly interacting with Lyst [49].

The observation that Nbeal2 localizes in the vicinity of the membrane, OCS and α-granules of platelets is compatible with its assumed role in membrane dynamics, and especially α-granule trafficking. Our results are supportive of the notion that the GEF Dock7 may be a critical intermediary in this membrane dynamics, which is also essential in the formation of platelets by MKs [46]. Therefore, the discovery that Dock7 is nearly depleted from platelets of GPS cases and *Nbeal2*$^{-/-}$ mice provides a plausible explanation why these platelets have an increased volume. In addition, our GWAS identified variants associated with platelet traits in nine genes encoding proteins in the Nbeal2 interactome (Nbeal2 itself, Dock7 and the seven circular orange nodes with appended gene names in Figure 1E). The variant rs60286666 in *DOCK7* is associated with the distribution width of platelet volume (p-value= 8.59×10^{-33}) providing further evidence of this Nbeal2 interactor possibly being important in the formation of platelets by MKs[39]. The role of Dock7 in platelet function has not been studied, but

From www.bloodjournal.org by guest on January 12, 2018. For personal use only.

the misty mouse, with a truncation in *Dock7*, has a prolonged bleeding time possibly explained by a reduced ability of platelets to support hemostasis [50]. The relevance of the canonical Rac1/Cdc42/Dock7 signaling pathway in megakaryopoiesis and platelet function has however been extensively studied. The conditional deletion of cofilin [51] and simultaneous deficiency of *Rac1* and *Cdc42* [52] result in decreased platelet count, larger platelets, and impairment of their function including defective shape change. Moreover, dysregulation of cofilin was also observed in a mouse knock-in and a family with type 2B von Willebrand disease, both presenting with macrothrombocytopenia [53]. Similar to these reports, we show that several elements of this signaling pathway, i.e. P-cofilin and Iqgap1 (a stabilizer of the active form of Cdc42 and Rac1) are dysregulated in murine *Nbeal2*$^{-/-}$ platelets, probably as a consequence of the reduced levels of Dock7. Hence, GTP-Rac1 levels are diminished in thrombin-stimulated *Nbeal2*$^{-/-}$ platelets, which show reduced actin polymerization and are unable to change shape efficiently (Figure 6D-H). Indeed, taken all the above evidence together, it is reasonable to assume that the macrothrombocytopenia in *Nbeal2*$^{-/-}$ mice and in GPS cases, is in part explained by the specific loss of Dock7.

Dock7 interacts with the PH-BEACH domain and this interaction seems to be diminished by all but one of the six GPS-causing mutations surveyed (Figure 3F). It has been suggested that Dock7 or one of its binding partners is localized in or on the surface of α-granules, and its PIP2/PIP3 binding domain makes the latter more likely [54]. Our results are supportive of this assumption and we reason that the interaction of Dock7 and α-granules is mediated through the BEACH domain.

From www.bloodjournal.org by guest on January 12, 2018. For personal use only.

Sec16a defines the budding sites on the ER membrane for trafficking of vesicles through the Golgi [55] and disruption of its binding to mutant WD40 domains (Figure 3B) could potentially affect platelet homeostasis. Similarly, changes in the function of Vac14, which in complex with Fig4 and Pikfyve (Figure 1H) regulates the levels of PI(3-5)P2, may alter endosomal trafficking and signaling [56].

In summary, from 129 binding partners of Nbeal2 identified by mass spectrometry, we have confirmed the interaction of three, Dock7, Sec16a and Vac14, by different biochemical and cellular approaches; and have also studied the functional relevance of one, Dock7, in platelet biology and its involvement in the abnormal formation of platelets by megakaryocytes in Gray Platelet Syndrome.

Acknowledgments

Research in the Ouwehand laboratory is supported by grants from the European Commission (BLUEPRINT Grant Code HEALTH-F5-2011-282510, HORIZON 2020 Grant Code 692041), National Institute for Health Research (NIHR; for funding of the Cambridge Biomedical Research Centre [RG64219]), Medical Research Council (WT098503), Bristol Myers-Squibb, British Heart Foundation (BHF; RP-PG-0310-1002 & RE/13/6/30180 for the BHF Cambridge Centre of Excellence) and NHS Blood and Transplant (NHSBT). The sequencing of the cases with GPS was supported by the NIHR BioResource (RBAG163); We thank Dr Kate Downes (University of Cambridge, UK), Professor Kathleen Freson (University of Leuven, Belgium) and Dr Keith Gomez (University College London, UK) for reviewing the sequencing results. TKB is the recipient of a Clinical Research Training Fellowship award from the British Society for Haematology and NHSBT, JCo is a Medical

From www.bloodjournal.org by guest on January 12, 2018. For personal use only.

Research Council Clinical Training Research fellow and WHO is a NIHR Senior Investigator.

Authorship

LM, MJ, SAH and JAG designed and performed experiments and analyzed data. MP, LY and JCh carried out proteomics analysis. JCo, TKB, LG, RP, SM, PAS and WJA analyzed data. PN performed EM of platelets. RF provided GPS samples. WWY carried out structural analysis. WHO and JAG wrote the manuscript.

Conflict-of-interest disclosure: The authors declare no competing financial interests.

From www.bloodjournal.org by guest on January 12, 2018. For personal use only.

References

1. Ruggeri ZM. Platelets in atherothrombosis. *Nat Med*. 2002;8(11):1227-1234.

2. Golebiewska EM, Poole AW. Platelet secretion: From haemostasis to wound healing and beyond. *Blood Rev*. 2015;29(3):153-162.

3. Gundelfinger ED, Kessels MM, Qualmann B. Temporal and spatial coordination of exocytosis and endocytosis. *Nat Rev Mol Cell Biol*. 2003;4(2):127-139.

4. de Saint Basile G, Menasche G, Fischer A. Molecular mechanisms of biogenesis and exocytosis of cytotoxic granules. *Nat Rev Immunol*. 2010;10(8):568-579.

5. De Matteis MA, Luini A. Mendelian disorders of membrane trafficking. *N Engl J Med*. 2011;365(10):927-938.

6. Patel SR, Hartwig JH, Italiano JE, Jr. The biogenesis of platelets from megakaryocyte proplatelets. *J Clin Invest*. 2005;115(12):3348-3354.

7. Jackson SP. Arterial thrombosis--insidious, unpredictable and deadly. *Nat Med*. 2011;17(11):1423-1436.

8. Nurden AT, Nurden P, Sanchez M, Andia I, Anitua E. Platelets and wound healing. *Front Biosci*. 2008;13:3532-3548.

9. Kisucka J, Butterfield CE, Duda DG, et al. Platelets and platelet adhesion support angiogenesis while preventing excessive hemorrhage. *Proc Natl Acad Sci U S A*. 2006;103(4):855-860.

10. Boilard E, Nigrovic PA, Larabee K, et al. Platelets amplify inflammation in arthritis via collagen-dependent microparticle production. *Science*. 2010;327(5965):580-583.

From www.bloodjournal.org by guest on January 12, 2018. For personal use only.

11. Semple JW, Italiano JE, Jr., Freedman J. Platelets and the immune continuum. *Nat Rev Immunol*. 2011;11(4):264-274.

12. Gay LJ, Felding-Habermann B. Contribution of platelets to tumour metastasis. *Nat Rev Cancer*. 2011;11(2):123-134.

13. Blair P, Flaumenhaft R. Platelet alpha-granules: basic biology and clinical correlates. *Blood Rev*. 2009;23(4):177-189.

14. Bariana TK, Ouwehand WH, Guerrero JA, et al. Dawning of the age of genomics for platelet granule disorders: improving insight, diagnosis and management. *Br J Haematol*. 2017;176(5):705-720.

15. Nagle DL, Karim MA, Woolf EA, et al. Identification and mutation analysis of the complete gene for Chediak-Higashi syndrome. *Nat Genet*. 1996;14(3):307-311.

16. Masliah-Planchon J, Darnige L, Bellucci S. Molecular determinants of platelet delta storage pool deficiencies: an update. *Br J Haematol*. 2013;160(1):5-11.

17. Castermans D, Volders K, Crepel A, et al. SCAMP5, NBEA and AMISYN: three candidate genes for autism involved in secretion of large dense-core vesicles. *Hum Mol Genet*. 2010;19(7):1368-1378.

18. Nuytens K, Tuand K, Di Michele M, et al. Platelets of mice heterozygous for neurobeachin, a candidate gene for autism spectrum disorder, display protein changes related to aberrant protein kinase A activity. *Mol Autism*. 2013;4(1):43.

19. Zufferey A, Schvartz D, Nolli S, Reny JL, Sanchez JC, Fontana P. Characterization of the platelet granule proteome: evidence of the presence of MHC1 in alpha-granules. *J Proteomics*. 2014;101:130-140.

20. Raccuglia G. Gray platelet syndrome. A variety of qualitative platelet disorder. *Am J Med*. 1971;51(6):818-828.

From www.bloodjournal.org by guest on January 12, 2018. For personal use only.

21. Albers CA, Cvejic A, Favier R, et al. Exome sequencing identifies NBEAL2 as the causative gene for gray platelet syndrome. *Nat Genet*. 2011;43(8):735-737.

22. Kahr WH, Hinckley J, Li L, et al. Mutations in NBEAL2, encoding a BEACH protein, cause gray platelet syndrome. *Nat Genet*. 2011;43(8):738-740.

23. Gunay-Aygun M, Falik-Zaccai TC, Vilboux T, et al. NBEAL2 is mutated in gray platelet syndrome and is required for biogenesis of platelet alpha-granules. *Nat Genet*. 2011;43(8):732-734.

24. Sowerby J, Thomas DC, Clare S, Espeli M, Guerrero JA, Hoenderdos K. Nbeal2 is required for neutrophil and NK cell function, and pathogen defence. *J Clin Invest*. 2017.

25. Drube S, Grimlowski R, Deppermann C, et al. The Neurobeachin-like 2 Protein Regulates Mast Cell Homeostasis. *J Immunol*. 2017;199(8):2948-2957.

26. Kahr WH, Lo RW, Li L, et al. Abnormal megakaryocyte development and platelet function in Nbeal2-/- mice. *Blood*. 2013;122(19):3349-3358.

27. Guerrero JA, Bennett C, van der Weyden L, et al. Gray platelet syndrome: proinflammatory megakaryocytes and alpha-granule loss cause myelofibrosis and confer metastasis resistance in mice. *Blood*. 2014;124(24):3624-3635.

28. Deppermann C, Cherpokova D, Nurden P, et al. Gray platelet syndrome and defective thrombo-inflammation in Nbeal2-deficient mice. *J Clin Invest*. 2013.

29. Cullinane AR, Schaffer AA, Huizing M. The BEACH is hot: a LYST of emerging roles for BEACH-domain containing proteins in human disease. *Traffic*. 2013;14(7):749-766.

30. Jogl G, Shen Y, Gebauer D, et al. Crystal structure of the BEACH domain reveals an unusual fold and extensive association with a novel PH domain. *EMBO J*. 2002;21(18):4785-4795.

From www.bloodjournal.org by guest on January 12, 2018. For personal use only.

31. Gebauer D, Li J, Jogl G, Shen Y, Myszka DG, Tong L. Crystal structure of the PH-BEACH domains of human LRBA/BGL. *Biochemistry*. 2004;43(47):14873-14880.

32. Pardo M, Lang B, Yu L, et al. An expanded Oct4 interaction network: implications for stem cell biology, development, and disease. *Cell Stem Cell*. 2010;6(4):382-395.

33. Vizcaino JA, Csordas A, del-Toro N, et al. 2016 update of the PRIDE database and its related tools. *Nucleic Acids Res*. 2016;44(D1):D447-456.

34. Nurden P, Jandrot-Perrus M, Combrie R, et al. Severe deficiency of glycoprotein VI in a patient with gray platelet syndrome. *Blood*. 2004;104(1):107-114.

35. Lentaigne C, Freson K, Laffan MA, et al. Inherited platelet disorders: toward DNA-based diagnosis. *Blood*. 2016;127(23):2814-2823.

36. Jupe S, Akkerman JW, Soranzo N, Ouwehand WH. Reactome - a curated knowledgebase of biological pathways: megakaryocytes and platelets. *J Thromb Haemost*. 2012;10(11):2399-2402.

37. Orchard S, Ammari M, Aranda B, et al. The MIntAct project--IntAct as a common curation platform for 11 molecular interaction databases. *Nucleic Acids Res*. 2014;42(Database issue):D358-363.

38. Petersen R, Lambourne JJ, Javierre BM, et al. Platelet function is modified by common sequence variation in megakaryocyte super enhancers. *Nat Commun*. 2017;8:16058.

39. Astle WJ, Elding H, Jiang T, et al. The Allelic Landscape of Human Blood Cell Trait Variation and Links to Common Complex Disease. *Cell*. 2016;167(5):1415-1429 e1419.

From www.bloodjournal.org by guest on January 12, 2018. For personal use only.

40. Javierre BM, Burren OS, Wilder SP, et al. Lineage-Specific Genome Architecture Links Enhancers and Non-coding Disease Variants to Target Gene Promoters. *Cell*. 2016;167(5):1369-1384 e1319.

41. Simeoni I, Stephens JC, Hu F, et al. A high-throughput sequencing test for diagnosing inherited bleeding, thrombotic, and platelet disorders. *Blood*. 2016;127(23):2791-2803.

42. Nurnberg ST, Rendon A, Smethurst PA, et al. A GWAS sequence variant for platelet volume marks an alternative DNM3 promoter in megakaryocytes near a MEIS1 binding site. *Blood*. 2012;120(24):4859-4868.

43. Chen L, Kostadima M, Martens JHA, et al. Transcriptional diversity during lineage commitment of human blood progenitors. *Science*. 2014;345(6204):1251033.

44. Bottega R, Nicchia E, Alfano C, et al. Gray platelet syndrome: Novel mutations of the NBEAL2 gene. *Am J Hematol*. 2017;92(2):E20-E22.

45. Bottega R, Pecci A, De Candia E, et al. Correlation between platelet phenotype and NBEAL2 genotype in patients with congenital thrombocytopenia and alpha-granule deficiency. *Haematologica*. 2013;98(6):868-874.

46. Aslan JE, McCarty OJ. Rho GTPases in platelet function. *J Thromb Haemost*. 2013;11(1):35-46.

47. Miyamoto Y, Yamauchi J. Cellular signaling of Dock family proteins in neural function. *Cell Signal*. 2010;22(2):175-182.

48. Malarkannan S, Awasthi A, Rajasekaran K, et al. IQGAP1: a regulator of intracellular spacetime relativity. *J Immunol*. 2012;188(5):2057-2063.

49. Tchernev VT, Mansfield TA, Giot L, et al. The Chediak-Higashi protein interacts with SNARE complex and signal transduction proteins. *Mol Med*. 2002;8(1):56-64.

From www.bloodjournal.org by guest on January 12, 2018. For personal use only.

50. Sviderskaya EV, Novak EK, Swank RT, Bennett DC. The murine misty mutation: phenotypic effects on melanocytes, platelets and brown fat. *Genetics*. 1998;148(1):381-390.

51. Bender M, Eckly A, Hartwig JH, et al. ADF/n-cofilin-dependent actin turnover determines platelet formation and sizing. *Blood*. 2010;116(10):1767-1775.

52. Pleines I, Dutting S, Cherpokova D, et al. Defective tubulin organization and proplatelet formation in murine megakaryocytes lacking Rac1 and Cdc42. *Blood*. 2013;122(18):3178-3187.

53. Kauskot A, Poirault-Chassac S, Adam F, et al. LIM kinase/cofilin dysregulation promotes macrothrombocytopenia in severe von Willebrand disease-type 2B. *JCI Insight*. 2016;1(16):e88643.

54. Cote JF, Motoyama AB, Bush JA, Vuori K. A novel and evolutionarily conserved PtdIns(3,4,5)P3-binding domain is necessary for DOCK180 signalling. *Nat Cell Biol*. 2005;7(8):797-807.

55. Cho HJ, Yu J, Xie C, et al. Leucine-rich repeat kinase 2 regulates Sec16A at ER exit sites to allow ER-Golgi export. *EMBO J*. 2014;33(20):2314-2331.

56. Jin N, Chow CY, Liu L, et al. VAC14 nucleates a protein complex essential for the acute interconversion of PI3P and PI(3,5)P(2) in yeast and mouse. *EMBO J*. 2008;27(24):3221-3234.

From www.bloodjournal.org by guest on January 12, 2018. For personal use only.

Figure legends

Figure 1. The Nbeal2 interactome. (A) Diagram showing the functional domains of Nbeal2 (ARM, Armadillo; ConA, Concanavalin A; WD40 repeat (WD40); PH, Pleckstrin homology; BEACH, Beige and Chediak Higashi domains). Construct 1 (PBW-FTAP) encompasses the PH, BEACH and amino-terminal WD40 domains and the FLAG Tandem Affinity Purification (FTAP) tag. Construct 2 (GFP-FTAP) encompasses Green Fluorescent Protein (GFP) and FTAP. (B) Ectopic expression of GFP-FTAP and PBW-FTAP in HEK. (C) FTAP-purification of GFP-FTAP and PBW-FTAP from HEK. Purified proteins were resolved by SDS-PAGE, visualized by blue Coomassie stain and analyzed by liquid chromatography-mass spectrometry. Some lanes in gels from panel B and C were deleted and replaced by black vertical lines. (D) Identified proteins (n=129) were classified according to their protein class using gene ontology terms. (E) Protein-protein interaction network (PPIN); 637 bait proteins representing the processes of hemostasis, megakaryopoiesis and platelet formation were used to retrieve 5,112 nodes (proteins) and 26,702 edges (biochemical reactions) by Reactome and IntAct. Orange nodes (n=91) are interactors present in the PPIN and the purple nodes (n=38) have interactions with one or more proteins of the PPIN. Nbeal2 is shown in black and Dock7, Sec16a, Vac14 are shown as orange triangles. (F-H) Subnetworks extracted from the PPIN in E for Dock7 (F), Sec16a (G) and Vac14 (H). The expression levels for the corresponding genes determined by the sequencing of RNA of human megakaryocytes (MKs) and expressed as $\log_2$ FPKM (Fragments Per Kilobase of transcript per Million mapped reads) is presented in white-to-green color and only nodes corresponding to genes with FPKM>1 in MKs are depicted (see color bar for relative FPKM values) [43].

From www.bloodjournal.org by guest on January 12, 2018. For personal use only.

The grey/black (1E-H), light blue (1F-1H) and dark blue (1F-1H) edges are based on the results of pulldown experiments reported in this study, Reactome and IntAct, respectively.

A Cytoscape file to generate an interactive version of the PPIN, containing gene expression levels and other annotation features is available from the data supplement.

Figure 2. Dock7, Sec16a and Vac14 interact with Nbeal2. (A-B) Immunoprecipitation (IP) of Dock7, Sec16a and Vac14 from PBW-FTAP HEK with total cell lysate (input) in A, IP results in B. PBW-FTAP was detected by anti-FLAG and a rabbit isotype IgG was used as control. Immunoblot with specific antibodies against Dock7, Sec16a and Vac14 (top blot in B). The other three blots in B show the specific binding of each of the cognate antibodies and the results with the isotype control immunoglobulin (ct-IgG) are in the first lane of the four blots in B. (C)-(E) Similar IP assays as in A carried out with HEK (C) or CHRF (D and E). (F) Proximity Ligation Assays (PLA) with human MKs showing the results for 1) αIIb and GPIX as negative control (top-left), 2) GPIbα and GPIX as positive control (top-middle), 3) Sec16a (top-right); Vac14 (two bottom-left); and Dock7 (two bottom-right), each interactor was tested in combination with Nbeal2. Interactions between proteins are presented as orange dots and cells were counterstained with Phalloidin (green) and DAPI (blue). 4) Quantitative analysis of the number of interactions per cell surface based on analysis of the PLA signals by Image Studio are presented in the bar graph. Comparisons were made against the negative control. Bars represent mean±SEM. * denotes p-value <0.05.

From www.bloodjournal.org by guest on January 12, 2018. For personal use only.

Figure 3. Effect of missense variants in the BEACH domain identified in Gray Platelet Syndrome cases on the interaction with Dock7 and Vac14. (A) Diagram representing the construct PB-FTAP including the PH and BEACH domains of Nbeal2 and the FTAP-tag. (B) HEK whole cell lysates containing a mixture of PB-FTAP and PBW-FTAP in a 1:1 ratio, or only PB-FTAP and PBW-FTAP (input) were immunoprecipitated (IP) using an isotype control IgG (Ct-IgG) or anti-FLAG. (C) Diagram representing the functional domains of Nbeal2 as per Figure 1A. Six amino acid mutations causative of Gray Platelet Syndrome (GPS) were selected on basis of their predicted functional consequences. (D) Computer model of the BEACH domain illustrating the six mutations shown in C and color-classified by disruptive effect. (E) PBW-FTAP in HEK expressing the reference allele or the six mutations were lysed (input), IP with anti-FLAG and blotted with anti-Vac14. Quantitation of the interaction Vac14-Nbeal2 for each of the variants and control was achieved by densitometry. (F) Similar assays performed in E but immunoblots were developed with anti-Dock7. Experiments were performed on five independent occasions. Bars represent mean±SEM. * denotes p-value<0.05.

Figure 4. Subcellular localization of PBW-FTAP and Nbeal2. (A) Ultrastructure of PBW-FTAP in CHRF by transmission electron microscopy (TEM). (B) High magnification of the area squared in A showing intracellular vesicles (V), mitochondria (M), Golgi and the nucleus (N). (C) Indirect gold-labeling of PBW-FTAP using anti-FLAG. Arrowheads point to clusters of gold across the cytoplasm of CHRF. (D) High magnification of the boxed area in C. (E) PBW-FTAP in CHRF stained as in C showing gold clusters in the cytoplasm but not in the intracellular vesicles. (F) High magnification of the boxed area in E. (G) Labeling of F-actin

From www.bloodjournal.org by guest on January 12, 2018. For personal use only.

filaments with Phalloidin (top panel), PBW-FTAP (middle panel) and overlay (bottom panel) of the results from top and middle panels, visualized by confocal microscopy; nucleus stained with DAPI. Scale bar represents 10 μm. (H) Gold-labeling of Nbeal2 in human platelets with rabbit antiserum. Gold particles label the platelet cytoplasm (arrowheads), α-granules (arrows), open canalicular system (circles) and periphery (flat ellipses). Images are representative of the results of two TEM, one (gold-labeling) and three (confocal microscopy) independent experiments.

Figure 5. Subcellular localization of Nbeal2 and its interactors, Dock7, Sec16a and Vac14 in platelets. (A) and (B) SDS-PAGE separated fractions 1-12 obtained by sucrose gradient centrifugation of human (A) and murine (B) platelets probed in immunoblots (IB) with specific antibodies against Nbeal2, Thbs1 (Thrombospondin-1), Crn (Calreticulin), Tuba1c (Tubulin Alpha 1c), and Actin (β-actin); for the murine platelets Crn was not probed but a specific antibody against Vegf (vascular endothelial growth factor) was included. (C)-(E) Localization of Nbeal2 interactors by IB in the different fractions obtained from platelets of control and *Nbeal2*$^{-/-}$ mice, (C) Dock7 in fraction 7-8 and fractions 3-4, respectively; (D) Sec16a in fraction 1-4; (E) Vac14 in fraction 5. (F) Levels of Nbeal2, Dock7, Sec16a and Vac14 in platelets from control and *Nbeal2*$^{-/-}$ mice. (G) Densitometry of the Western blot results shown in F; total lysates from F were performed on platelets of at least 4 (Nbeal2, Sec16a, Vac14) and 8 (Dock7) mice per genotype group. (H) Levels of Dock7 in platelets from Gray Platelet Syndrome (GPS) cases. For experiments in (G) and (H) Gapdh was used as a loading control and levels of the other proteins were normalized to Gapdh. Bars represent mean±SEM. * denotes p-value<0.05.

From www.bloodjournal.org by guest on January 12, 2018. For personal use only.

Figure 6. The Dock7 signaling pathway is altered in *Nbeal2*$^{-/-}$ platelets. (A) Platelet lysates from control and *Nbeal2*$^{-/-}$ mice were resolved by SDS-PAGE and expression levels of Rac1, Cdc42, cofilin, P-cofilin, Iqgap1, Pdxp and Gapdh were observed by immunoblot (IB) with specific antibodies. (B) Densitometry of the results of the blots shown in A using Image Studio. (C) and (D) Time course of active Cdc42 (GTP-Cdc42) and active Rac1 (GTP-Rac1) in platelets stimulated with 0.5 U/mL thrombin. (E) F-actin levels in resting and thrombin-activated platelets. (F) Relative increase in F-actin levels in thrombin-activated *vs* resting platelets of control and *Nbeal2*$^{-/-}$ mice. (G) Representative images of platelets spreading on fibrinogen in response to thrombin from control and *Nbeal2*$^{-/-}$ mice at different magnifications. (H) Quantitation of fully spread and round platelets from control and *Nbeal2*$^{-/-}$ mice in response to activation with thrombin or ADP. Platelets in five random fields per condition were counted, with each field having between 80-120 platelets; four animals per genotype group were used. Bars represent mean±SEM. *, ** and *** denote p-values <0.05, <0.005 and <0.0005, respectively.

Figure 1

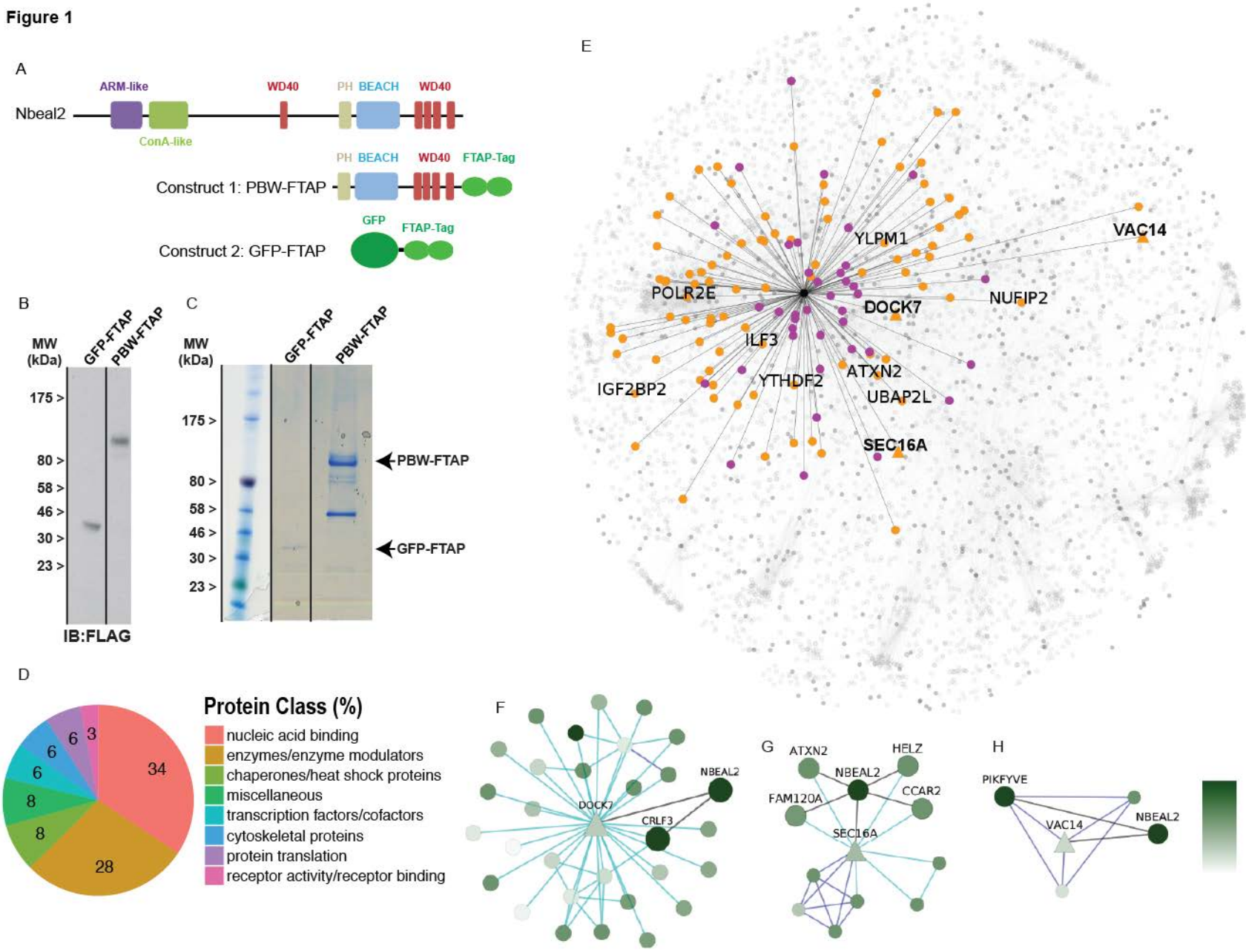
A
ARM-like
WD40
PH
BEACH
WD40
Nbeal2
ConA-like
PH
BEACH
WD40
FTAP-Tag
Construct 1: PBW-FTAP
GFP
FTAP-Tag
Construct 2: GFP-FTAP
B
MW (kDa)
GFP-FTAP
PBW-FTAP
175 >
80 >
58 >
46 >
30 >
23 >
IB:FLAG
C
MW (kDa)
GFP-FTAP
PBW-FTAP
175 >
80 >
58 >
46 >
30 >
23 >
PBW-FTAP
GFP-FTAP
D
Protein Class (%)
nucleic acid binding
enzymes/enzyme modulators
chaperones/heat shock proteins
miscellaneous
transcription factors/cofactors
cytoskeletal proteins
protein translation
receptor activity/receptor binding
34
28
8
8
6
6
6
3
E
YLPM1
VAC14
POLR2E
DOCK7
NUFIP2
ILF3
ATXN2
YTHDF2
IGF2BP2
UBAP2L
SEC16A
F
NBEAL2
DOCK7
CRLF3
G
ATXN2
HELZ
NBEAL2
FAM120A
CCAR2
SEC16A
H
PIKFYVE
VAC14
NBEAL2

Figure 2

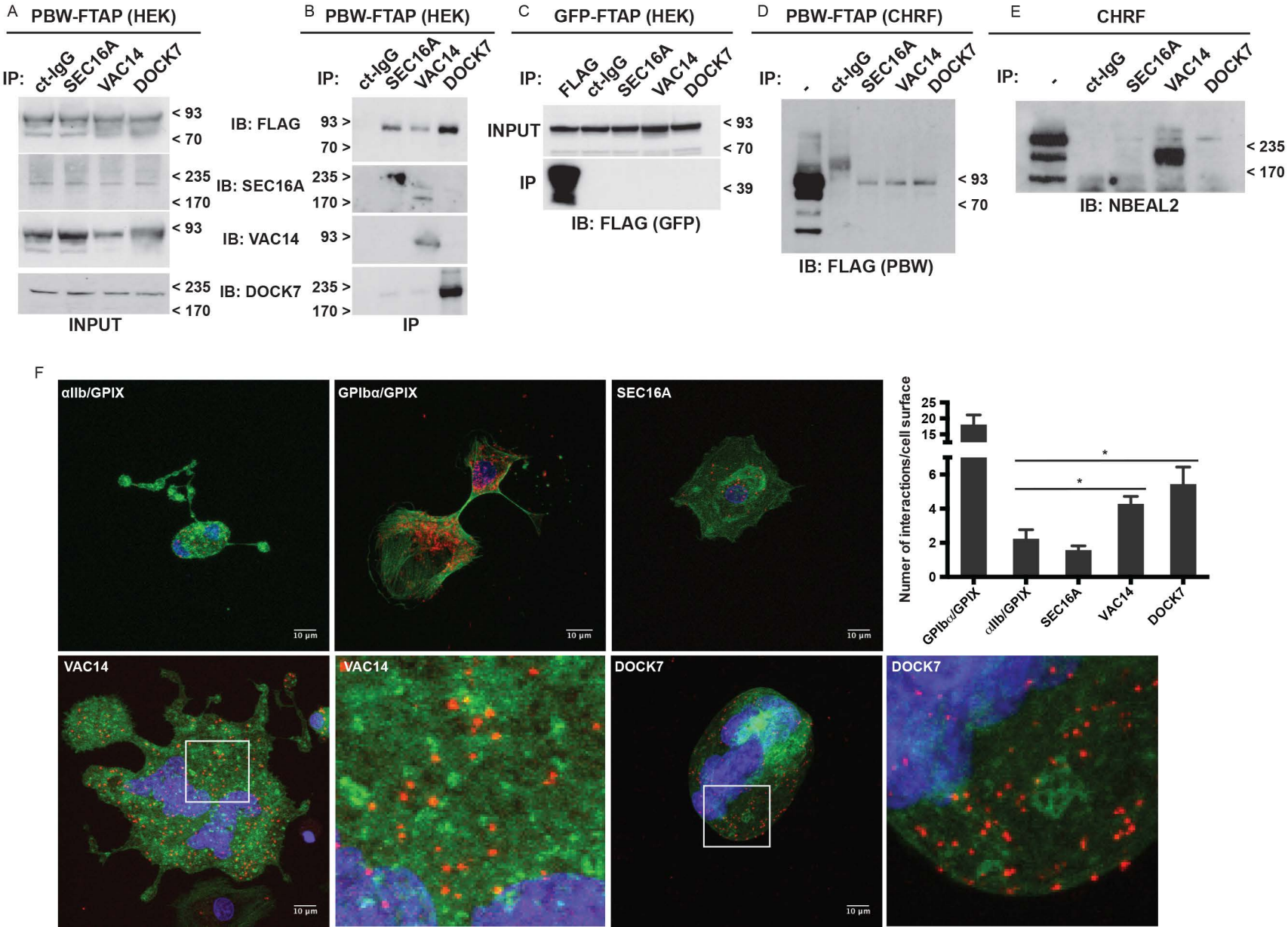
A
PBW-FTAP (HEK)
IP: ct-IgG SEC16A VAC14 DOCK7
< 93
< 70
< 235
< 170
< 93
< 235
< 170
INPUT
IB: FLAG
IB: SEC16A
IB: VAC14
IB: DOCK7
93 >
70 >
235 >
170 >
93 >
235 >
170 >
IP
B
PBW-FTAP (HEK)
IP: ct-IgG SEC16A VAC14 DOCK7
C
GFP-FTAP (HEK)
IP: FLAG ct-IgG SEC16A VAC14 DOCK7
INPUT
IP
< 93
< 70
< 93
< 39
IB: FLAG (GFP)
D
PBW-FTAP (CHRF)
IP: - ct-IgG SEC16A VAC14 DOCK7
< 93
< 70
IB: FLAG (PBW)
E
CHRF
IP: - ct-IgG SEC16A VAC14 DOCK7
< 235
< 170
IB: NBEAL2
F
αIIb/GPIX
GPIbα/GPIX
SEC16A
10 μm
Numer of interactions/cell surface
25
20
15
6
4
2
0
*
*
GPIbα/GPIX
αIIb/GPIX
SEC16A
VAC14
DOCK7
VAC14
VAC14
DOCK7
DOCK7
10 μm

Figure 3

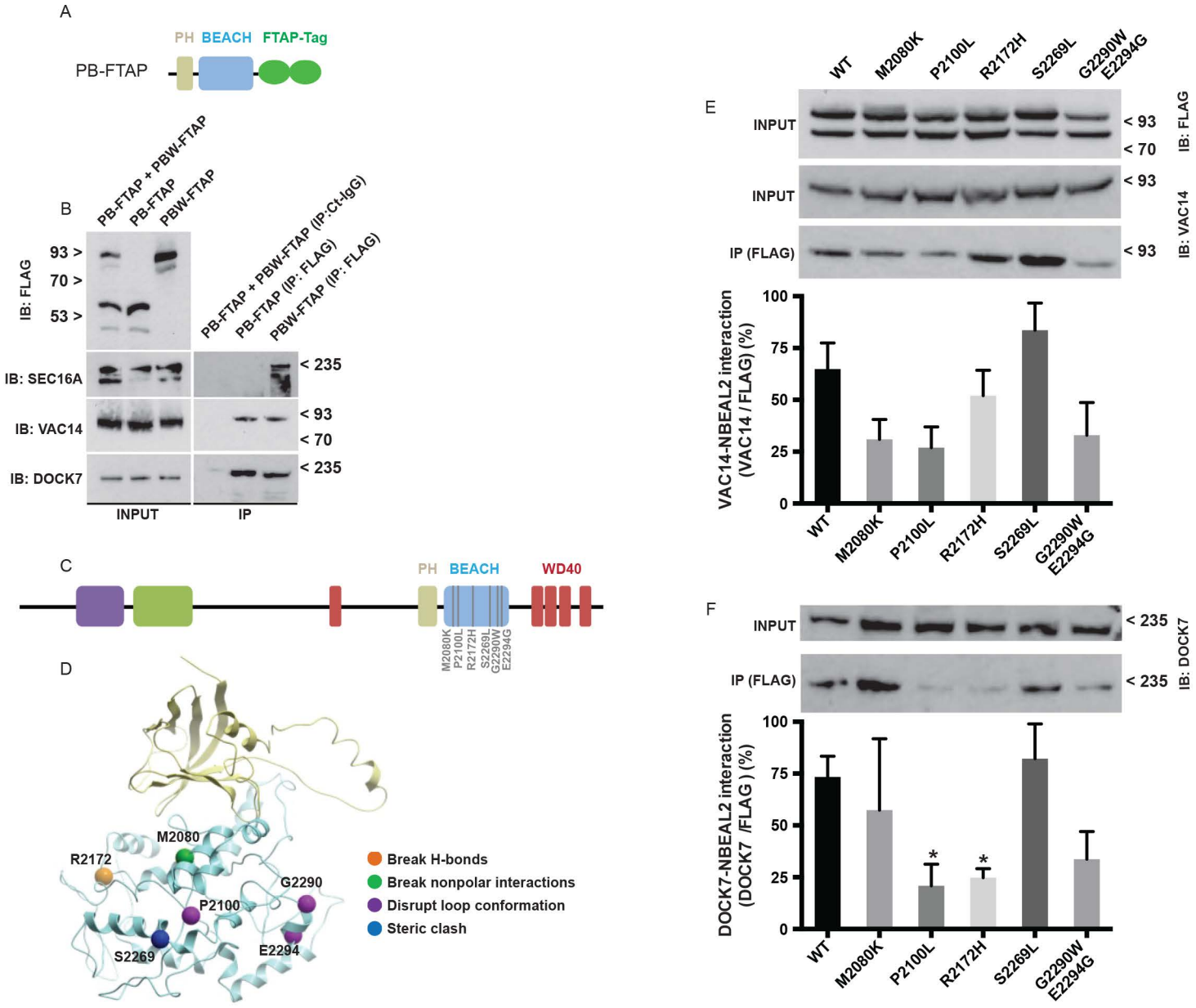
A
PH BEACH FTAP-Tag
PB-FTAP
B
PB-FTAP + PBW-FTAP
PB-FTAP
PBW-FTAP
IB: FLAG
93 >
70 >
53 >
PB-FTAP + PBW-FTAP (IP:Ct-IgG)
PB-FTAP (IP: FLAG)
PBW-FTAP (IP: FLAG)
IB: SEC16A
< 235
IB: VAC14
< 93
< 70
IB: DOCK7
< 235
INPUT
IP
C
PH
BEACH
WD40
M2080K
P2100L
R2172H
S2269L
G2290W
E2294G
D
M2080
R2172
G2290
P2100
S2269
E2294
Break H-bonds
Break nonpolar interactions
Disrupt loop conformation
Steric clash
E
WT
M2080K
P2100L
R2172H
S2269L
G2290W
E2294G
INPUT
< 93
< 70
IB: FLAG
INPUT
< 93
IB: VAC14
IP (FLAG)
< 93
VAC14-NBEAL2 interaction
(VAC14 / FLAG) (%)
100
75
50
25
0
F
INPUT
< 235
IP (FLAG)
< 235
IB: DOCK7
DOCK7-NBEAL2 interaction
(DOCK7 /FLAG) (%)
100
75
50
25
0
*
*

Figure 4

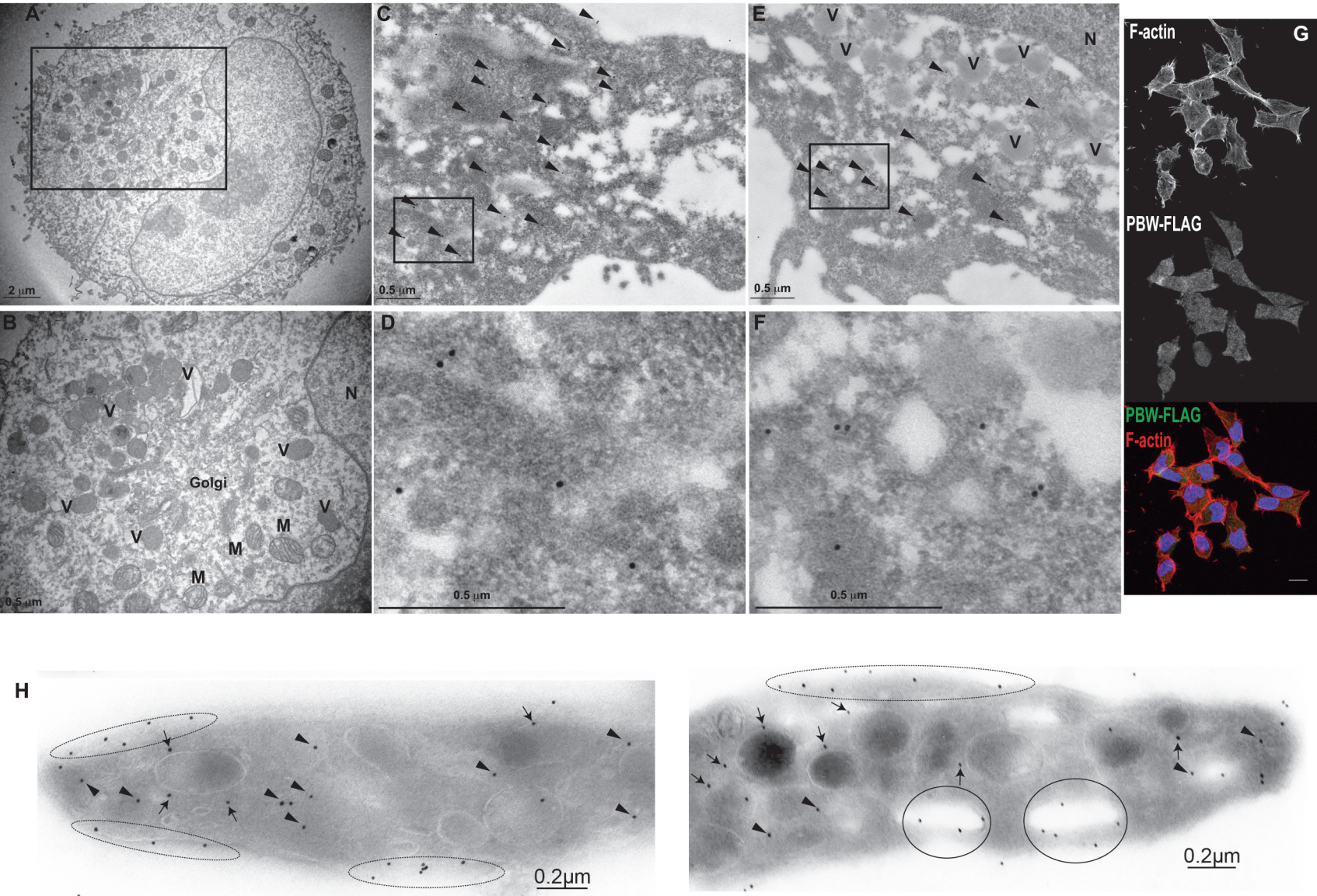
A
2 μm
B
V
N
V
V
Golgi
V
V
V
M
M
M
0.5 μm
C
0.5 μm
D
0.5 μm
E
V
V
V
V
N
V
V
0.5 μm
F
0.5 μm
G
F-actin
PBW-FLAG
PBW-FLAG
F-actin
H
0.2μm
0.2μm

Figure 5

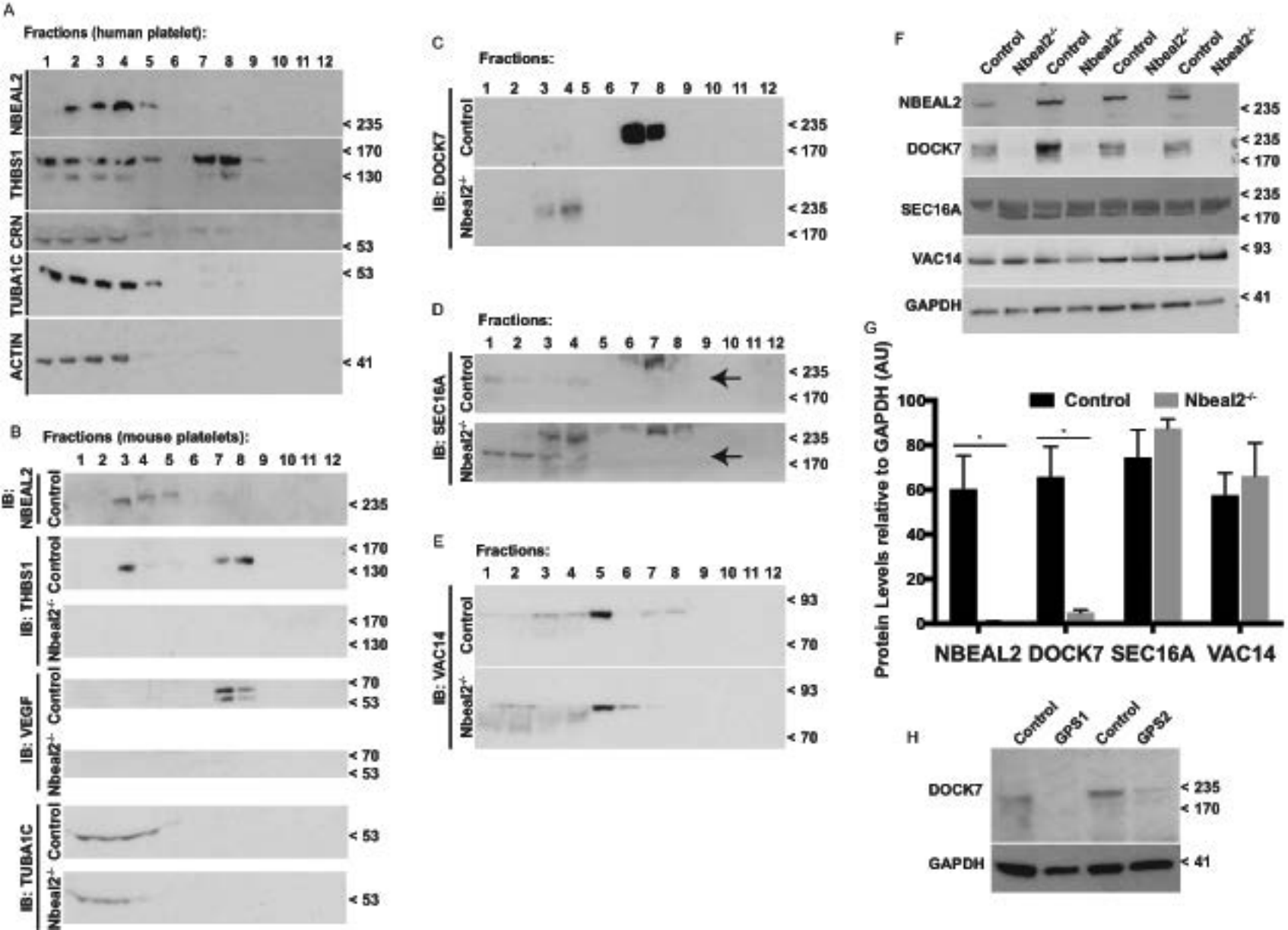
A
Fractions (human platelet):
1 2 3 4 5 6 7 8 9 10 11 12
NBEAL2
THBS1
CRN
TUBA1C
ACTIN
< 235
< 170
< 130
< 53
< 53
< 41
B
Fractions (mouse platelets):
1 2 3 4 5 6 7 8 9 10 11 12
IB: NBEAL2 Control
IB: THBS1 Control
Nbeal2-/-
IB: VEGF Control
Nbeal2-/-
IB: TUBA1C Control
Nbeal2-/-
< 235
< 170
< 130
< 170
< 130
< 70
< 53
< 70
< 53
< 53
< 53
C
Fractions:
1 2 3 4 5 6 7 8 9 10 11 12
IB: DOCK7 Control
Nbeal2-/-
< 235
< 170
< 235
< 170
D
Fractions:
1 2 3 4 5 6 7 8 9 10 11 12
IB: SEC16A Control
Nbeal2-/-
< 235
< 170
< 235
< 170
E
Fractions:
1 2 3 4 5 6 7 8 9 10 11 12
IB: VAC14 Control
Nbeal2-/-
< 93
< 70
< 93
< 70
F
Control Nbeal2-/- Control Nbeal2-/- Control Nbeal2-/- Control Nbeal2-/-
NBEAL2
DOCK7
SEC16A
VAC14
GAPDH
< 235
< 235
< 170
< 235
< 170
< 93
< 41
G
Protein Levels relative to GAPDH (AU)
100
80
60
40
20
0
Control
Nbeal2-/-
*
*
NBEAL2 DOCK7 SEC16A VAC14
H
Control GPS1 Control GPS2
DOCK7
GAPDH
< 235
< 170
< 41

Figure 6

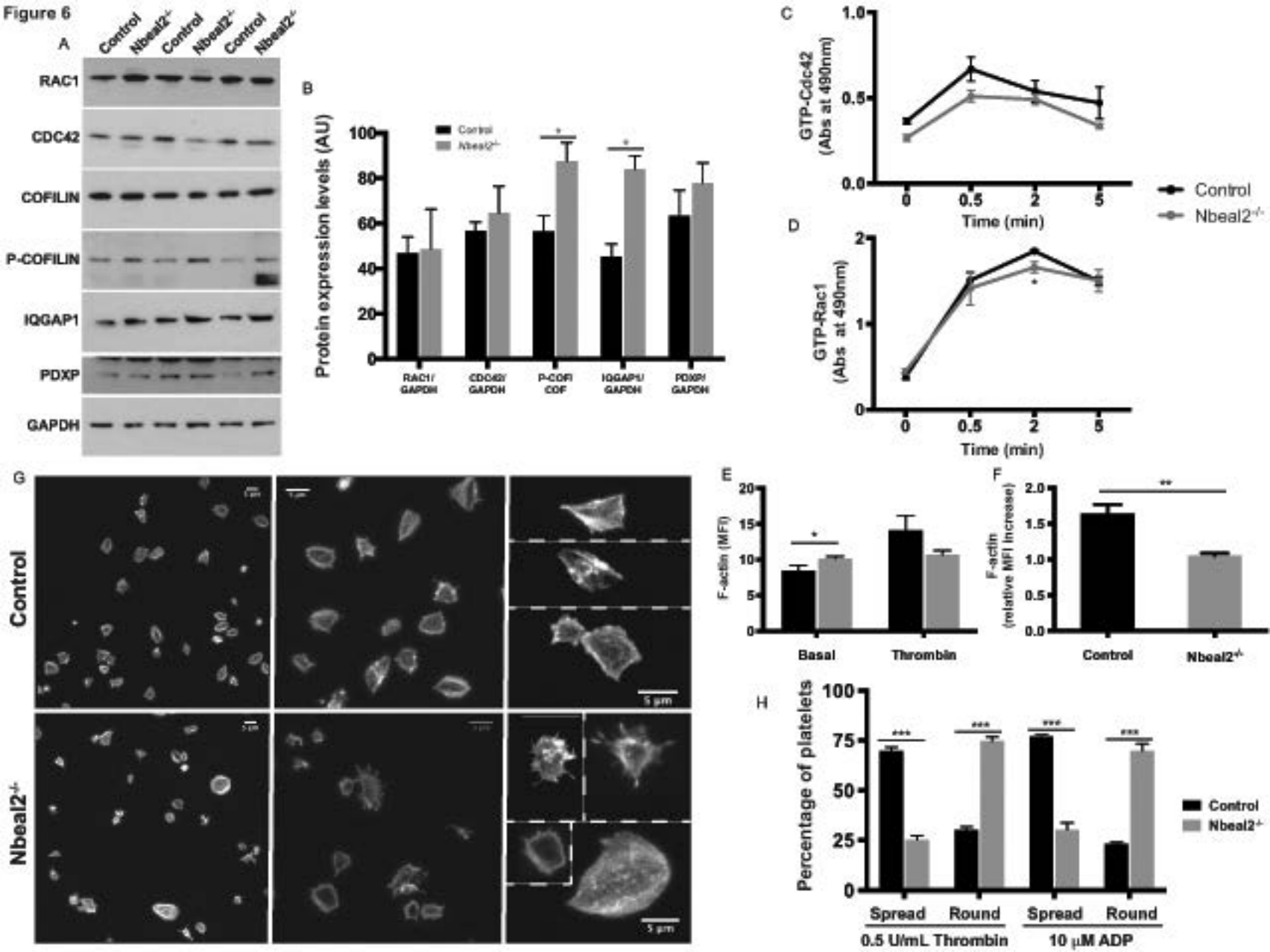
A
Control
Nbeal2-/-
RAC1
CDC42
COFILIN
P-COFILIN
IQGAP1
PDXP
GAPDH
B
Protein expression levels (AU)
Control
Nbeal2-/-
RAC1/ GAPDH
CDC42/ GAPDH
P-COFI COF
IQGAP1/ GAPDH
PDXP/ GAPDH
C
GTP-Cdc42 (Abs at 490nm)
Time (min)
Control
Nbeal2-/-
D
GTP-Rac1 (Abs at 490nm)
Time (min)
E
F-actin (MFI)
Basal
Thrombin
F
F-actin (relative MFI increase)
Control
Nbeal2-/-
G
Control
Nbeal2-/-
5 µm
H
Percentage of platelets
Spread
Round
Spread
Round
0.5 U/mL Thrombin
10 µM ADP
Control
Nbeal2-/-

From www.bloodjournal.org by guest on January 12, 2018. For personal use only.

Prepublished online November 29, 2017;
doi:10.1182/blood-2017-08-800359

The BEACH-domain containing protein, Nbeal2, interacts with Dock7, Sec16a and Vac14

Louisa Mayer, Maria Jasztal, Mercedes Pardo, Salvadora Aguera de Haro, Janine Collins, Tadbir K. Bariana, Peter A. Smethurst, Luigi Grassi, Romina Petersen, Paquita Nurden, Rémi Favier, Lu Yu, Stuart Meacham, William J. Astle, Jyoti Choudhary, Wyatt W. Yue, Willem H. Ouwehand and Jose A. Guerrero

Information about reproducing this article in parts or in its entirety may be found online at:
http://www.bloodjournal.org/site/misc/rights.xhtml#repub_requests

Information about ordering reprints may be found online at:
http://www.bloodjournal.org/site/misc/rights.xhtml#reprints

Information about subscriptions and ASH membership may be found online at:
http://www.bloodjournal.org/site/subscriptions/index.xhtml

Advance online articles have been peer reviewed and accepted for publication but have not yet appeared in the paper journal (edited, typeset versions may be posted when available prior to final publication). Advance online articles are citable and establish publication priority; they are indexed by PubMed from initial publication. Citations to Advance online articles must include digital object identifier (DOIs) and date of initial publication.

Blood (print ISSN 0006-4971, online ISSN 1528-0020), is published weekly by the American Society of Hematology, 2021 L St, NW, Suite 900, Washington DC 20036.
Copyright 2011 by The American Society of Hematology; all rights reserved.